DALTON
FULL PAPER

A detailed NMR study of the solution stereodynamics in tricarbonylrhenium(I) halide complexes of the non-racemic chiral ligand 2,6-bis[(4*R*,5*R*)-dimethyl-1,3-dioxan-2-yl]pyridine (L^1) and the molecular structure of *fac*-[$ReBr(CO)_3(L^1)$] †

Peter J. Heard,*[a] Paul M. King,[a] Alex. D. Bain,[b] Paul Hazendonk[b] and Derek A. Tocher[c]

[a] *Department of Chemistry, Birkbeck University of London, 29 Gordon Square, London, UK WC1H 0PP. E-mail: p.heard@chemistry.bbk.ac.uk*
[b] *Department of Chemistry, McMaster University, 1280 Main Street West, Hamilton, Ontario L8S 4M1, Canada*
[c] *Department of Chemistry, University College London, Christopher Ingold Laboratories, 20 Gordon Street, London, UK WC1H 0AJ*

Received 19th May 1999, Accepted 11th November 1999

Tricarbonylrhenium(I) halide complexes of the non-racemic chiral ligand 2,6-bis[(4*R*,5*R*)-dimethyl-1,3-dioxan-2-yl]pyridine (L^1), namely *fac*-[$ReX(CO)_3(L^1)$] (X = Cl, Br or I), have been prepared. In these complexes the ligand is bound in a bidentate fashion, with the N atom of the pyridine ring and an O atom of one of the acetal rings co-ordinated to the octahedral metal centre. The bidentate mode is confirmed by the crystal structure of *fac*-[$ReBr(CO)_3(L^1)$]. There are four possible diastereoisomers, depending on the configuration at the metal centre and at the acetal-carbon atom of the co-ordinated ring; the crystal structure of *fac*-[$ReBr(CO)_3(L^1)$] shows that the *SR* diastereoisomer is present in the solid-state. In solution, three of the four possible diastereoisomers are observed, namely *SR*, *RR* and *SS*; their relative populations are in the order *SR* > *RR* > *SS*. Above ambient temperature the complexes are stereochemically non-rigid. The fluxional kinetics have been measured by a combination of standard band shape analysis and selective inversion experiments. Two distinct processes are present: an acetal *ring flip* and exchange of the pendant and co-ordinated acetal rings. The latter process occurs *via* two independent mechanisms, namely *tick-tock* and *rotation* pathways. The activation energies for the stereodynamics are in the ranges 72–73 kJ mol^{-1} (*tick-tock*), 77–78 kJ mol^{-1} (acetal *ring flip*) and 83–90 kJ mol^{-1} (*rotation*) at 298 K.

Introduction

Transition metal complexes of ligands that possess redundant donor atoms are potentially fluxional.[1] Recent work by our group has focused on the study of dynamic stereochemical rearrangements in complexes of non-racemic chiral nitrogen donor ligands, such as 2,6-bis[(4*S*)-alkyloxazolin-2-yl]pyridine (alkyl = methyl or isopropyl).[2,3] The chiral centres on the ligand provide an excellent spectroscopic handle on the mechanism(s) of the fluxions and enable pathways that are otherwise 'invisible' to be elucidated. This paper details the results of studies on the solution stereodynamics of the tricarbonylrhenium(I) halide complexes of the closely related O/N/O hybrid ligand 2,6-bis[(4*R*,5*R*)-dimethyl-1,3-dioxan-2-yl]pyridine (L^1), namely *fac*-[$ReX(CO)_3(L^1)$] (X = Cl, Br or I).

When co-ordinated to a metal centre in a bidentate fashion, potentially (*mer*) terdentate ligands, such as 2,2′:6′,2″-terpyridine (terpy)[4–6] are fluxional; pendant and bound donor groups are exchanged. We demonstrated recently that there are two independent mechanisms *via* which this occurs in systems of like donor atoms (N/N/N), namely a *tick-tock* pathway and a *rotational* pathway.[2] As would be expected, the energetics of these mechanisms are dependent on the nature of the ligand substiuents.[2,3] The question now arises as to the influence of different donor atoms on the stereodynamics. We therefore chose to investigate the tricarbonylrhenium(I) halide complexes of the chiral non-racemic ligand 2,6-bis[(4*R*,5*R*)-dimethyl-1,3-dioxan-2-yl]pyridine (L^1), which undergo similar structural dynamics. Furthermore, these complexes also exhibit reversible 'flip' of the co-ordinated acetal ring,[7] leading to highly complex solution stereodynamics. The asymmetric centres enable the various stereodynamic processes to be elucidated, demonstrating clearly the power of using non-racemic chiral ligands for the measurement of fluxional kinetics.

† *Supplementary data available*: rotatable 3-D crystal structure diagram in CHIME format. See http://www.rsc.org/suppdata/dt/1999/4495/

Experimental

Syntheses

All procedures were carried out under an atmosphere of dry, oxygen-free nitrogen using standard Schlenk techniques. Solvents were dried[8] and degassed before use. The starting materials, purchased from Aldrich Chemical Company, were used without further purification. The pentacarbonylrhenium(I) halides were prepared by standard methods.[9] The ligand, 2,6-bis[(4*R*,5*R*)-dimethyl-1,3-dioxan-2-yl]pyridine (L^1)[10] and the complexes *fac*-[$ReX(CO)_3(L^1)$] (X = Cl, Br or I) were prepared as described below. Analytical data are reported in Table 1.

2,6-Bis[(4*R*,5*R*)-dimethyl-1,3-dioxan-2-yl]pyridine (L^1). 2,6-Pyridinedicarboxaldehyde (1.0 g, 7.4 mmol), (2*R*,3*R*)-butanediol (1.7 cm^3, 18.6 mmol), 2,2-dimethoxypropane (1.0 cm^3, 10.7 mmol), and *para*-toluenesulfonic acid (*ca*. 40 mg) were refluxed for 72 hours in 30 cm^3 of toluene. The resulting solution was extracted with an aqueous sodium carbonate solution (3 × 30 cm^3) then water (3 × 30 cm^3), dried over $MgSO_4$, and concen-

Table 1 Analytical data for the complexes $[ReX(CO)_3(L^1)]$

Complex	Yield[a] (%)	Infrared data[b]/ cm^{-1}	Mass spectral data[c]	Analyses[d](%) C	H	N
$[ReCl(CO)_3(L^1)]$	74	2033, 1923, 1902	484 $[M - PR]^+$, 449 $[M - PR - Cl]^+$	36.67(36.96)	3.53(3.62)	2.39(2.39)
$[ReBr(CO)_3(L^1)]$	91	2033, 1924, 1904	528 $[M - PR]^+$, 500 $[M - PR - CO]^+$, 449 $[M - PR - Br]^+$	33.88(34.35)	3.08(3.36)	2.18(2.22)
$[ReI(CO)_3(L^1)]$	53	2032, 1925, 1907	576 $[M - PR]^+$, 548 $[M - PR - CO]^+$, 449 $[M - PR - Cl]^+$	31.62(31.96)	2.94(3.13)	2.04(2.07)

[a] Percentage yield relative to $[ReX(CO)_5]$. [b] Carbonyl stretching modes; spectra recorded in CH_2Cl_2 solution. [c] LSIMS technique; PR = pendant acetal ring. [d] Calculated values in parentheses.

trated to dryness *in vacuo*. The solid residue was purified by crystallisation from hot hexane. Yield: 1.5 g, 72%.

Complexes $[ReX(CO)_3(L^1)]$ (X = Cl, Br or I). In a typical experiment, *ca*. 0.25 mmol of the appropriate pentacarbonylrhenium(I) halide was refluxed for *ca*. 18 hours with a small excess of the ligand (L^1) in 20 cm^3 of benzene. The benzene was then removed *in vacuo*. The solid residue was crystallised from CH_2Cl_2–hexane solution at −20 °C to yield pure, crystalline $[ReX(CO)_3(L^1)]$.

Physical methods

Solution ^1H NMR spectra were acquired on either Bruker AM300 or AMX600 Fourier transform spectrometers, operating at 300.13 and 600.13 MHz, respectively. Spectra were recorded in $(CDCl_2)_2$ or $CDCl_3$ solution. Chemical shifts are reported in ppm relative to tetramethylsilane as an internal standard. Probe temperatures were controlled by standard B-VT 2000 units and are considered accurate to within ±1 °C. Variable temperature experiments were carried out in the temperature range 298–393 K; probe temperatures were allowed to equilibrate for *ca*. 15 minutes prior to the acquisition of each spectrum. Band shapes were analysed using the non-iterative simulation program MEX.[11] Inversion–recovery experiments were carried out using our program INVREC2P (modified from the Bruker automation program INVREC), which generates the pulse sequence *D*1–90°–τ–90°–variable delay–90°–free induction decay. For the non-selective experiments (measurement of T_1) τ was 10 μs. For the selective experiments the signal to be inverted was placed on resonance and τ was $1/2\Delta\nu$ ($\Delta\nu$ is the separation of the inverted and observed signals in Hz). The relaxation delay, *D*1, was 30 s. 12–16 and 24–30 experiments (*i.e*. the number of delays in the VD list) were carried out for the non-selective and selective inversions, respectively. Exchange rates were extracted from the longitudinal magnetisations using the program CIFIT.[12] The rate constants obtained from the dynamic NMR spectra were used to calculate the Eyring activation parameters; the errors quoted are those defined by Binsch and Kessler.[13] Two-dimensional exchange (EXSY) spectra were acquired using the Bruker automation program NOESYTP, which generates the program *D*1–90°–*D*0–90°–*D*8–90°–free induction decay. Typical acquisition parameters for the EXSY experiment are described elsewhere.[3] Exchange rates from the EXSY experiment were extracted from the two-dimensional intensity matrix (determined by volume integration) using the program D2DNMR.[14]

Geometric calculations were carried out using the Molden program.[15] Diastereoisomers were constructed using the data obtained from the crystal structure determination of $[ReBr(CO)_3(L^1)]$ and close contact distances were measured between the metal moiety and the co-ordinated acetal ring. Infrared spectra were obtained as CH_2Cl_2 solutions on a Nicolet 205 FT-IR spectrometer, operating in the region 4000–400 cm^{-1}. Mass spectra (LSIMS) were recorded at the London School of Pharmacy on a VG Analytical ZAB-SE4F instrument, using Xe^+ ion bombardment at 8 kV energy. Elemental analyses were performed at University College London.

Crystallography

A single crystal of $[ReBr(CO)_3(L^1)]$ of approximate dimensions $0.78 \times 0.72 \times 0.44$ mm was obtained as described above and mounted on a glass fibre. Geometric and intensity data were obtained from this sample using an automatic four-circle Nicolet R3mV diffractometer, using the ω–2θ technique at 293(2) K. Three standard reflections remeasured every 97 scans, showed no significant loss of intensity during data collection.

Crystal data and data collection parameters. $C_{18}H_{21}BrNO_7Re$, $M = 629.47$, monoclinic, space group $P2_1$, Mo-Kα radiation ($\lambda = 0.71073$ Å), $a = 9.231(2)$, $b = 11.296(2)$, $c = 10.975(2)$ Å, $U = 1099.7(4)$ Å^3, $Z = 2$, $D_c = 1.901$ mg m^{-3}, $\mu = 7.378$ mm^{-1}, $F(000) = 604$, data collection range $2.56 \leq \theta \leq 25.29°$, 4083 reflections collected, 3832 unique ($R_{int} = 0.0516$).

Structure solution and refinement. The structure was solved by direct methods and refined to convergence by least-squares (SHELXL 93).[16] The final cycle of least-squares included 253 parameters for the 3826 variables. The final R and $wR2$ values were 0.0435 and 0.1082, respectively [$I > 2\sigma(I)$, 3501 data], and 0.0508 and 0.1225 for all data. The absolute configuration was determined unambiguously using SHELXL 93 procedures; calculated Flack parameter −0.07(2).

CCDC reference number 186/1732.

See http://www.rsc.org/suppdata/dt/1999/4495/ for crystallographic files in .cif format.

Results and discussion

The tricarbonylrhenium(I) halide complexes of the non-racemic chiral ligand, 2,6-bis[(4*R*,5*R*)-dimethyl-1,3-dioxan-2-yl]pyridine (L^1), namely *fac*-$[ReX(CO)_3(L^1)]$ (X = Cl, Br or I), were prepared as described and isolated as air-stable crystalline solids. The infrared spectra of the complexes display three carbonyl stretching bands in the region 1850–2050 cm^{-1}, characteristic of a facial tricarbonyl metal moiety.[17] Elemental analyses (C, H, and N) are consistent with the formulated species. The mass spectra (LSIMS) do not show any peaks due to the molecular species, $[M]^+$. In each case the highest mass peak corresponds to loss of the pendant acetal ring and the most intense peaks were observed at $m/z^+ = 449$, due to loss of the halogen (X = Cl, Br or I) from this species. In all cases the observed and calculated isotope patterns are fully consistent. Analytical data are reported in Table 1. Analytical and spectroscopic data indicate clearly that the ligand co-ordinates to the metal in a bidentate fashion *via* the nitrogen donor of the pyridine ring and an oxygen donor of one of the acetal rings. The bidentate bonding

Table 2 Selected bond lengths (Å) and angles (°) for [ReBr(CO)$_3$(L^1)] with estimated standard deviations in parentheses

Re(1)–O(1)	2.225(8)	O(2)–C(3)	1.44(2)
Re(1)–N(1)	2.292(10)	C(2)–C(3)	1.54(2)
Re(1)–Br(1)	2.629(2)	O(3)–C(11)	1.43(2)
Re(1)–C(30)	1.90(2)	O(3)–C(13)	1.45(2)
O(1)–C(2)	1.49(2)	O(4)–C(11)	1.41(2)
O(1)–C(5)	1.467(14)	O(4)–C(14)	1.48(2)
O(2)–C(5)	1.41(2)	C(13)–C(14)	1.53(2)
C(40)–Re(1)–C(20)	83.8(9)	N(1)–Re(1)–Br(1)	85.4(2)
C(20)–Re(1)–N(1)	104.3(5)	C(5)–O(1)–Re(1)	116.6(7)
O(1)–Re(1)–N(1)	74.6(3)	C(6)–N(1)–Re(1)	114.1(8)
O(1)–Re(1)–C(40)	97.3(8)	O(1)–C(5)–C(6)	110.8(10)
O(1)–Re(1)–C(30)	93.9(5)	C(2)–O(1)–C(5)	107.8(9)
N(1)–Re(1)–C(30)	91.7(4)	O(1)–C(5)–O(2)	105.5(9)
O(1)–Re(1)–Br(1)	84.9(2)	O(3)–C(11)–O(4)	107.2(10)

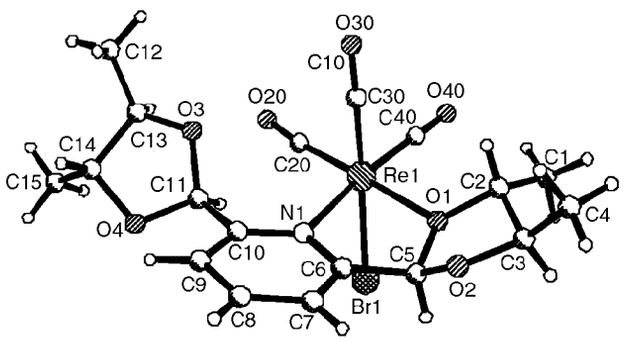

Fig. 1 Molecular structure of *fac*-[ReBr(CO)$_3$(L^1)] showing the atom numbering scheme.

is confirmed by the crystal structure of *fac*-[ReBr(CO)$_3$(L^1)] (see below).

Crystal structure of *fac*-[ReBr(CO)$_3$(L^1)]

Fig. 1 shows the molecular structure of [ReBr(CO)$_3$(L^1)] {L^1 = 2,6-bis[(4*R*,5*R*)-dimethyl-1,3-dioxan-2-yl]pyridine}. Selected bond lengths and angles are reported in Table 2. The structure was obtained to confirm the bidentate bonding mode of the ligand and to determine unambiguously the absolute configuration. Fig. 1 shows clearly that the ligand is acting in a bidentate fashion *via* the pyridine N donor and an acetal O donor, and the absolute configuration (*R*) at C(2), C(3), C(13), and C(14) is confirmed. The configuration at the metal,[7,18] determined by viewing the molecule down the pseudo C_3 axis of symmetry (CO ligands down) and assigning priorities to the three remaining donor atoms (Br, O, and N) according to the Cahn–Ingold–Prelog system,[19] is *S* and the configuration at the acetal-carbon atom of the co-ordinated ring C(5) is *R*.

The geometry at the metal centre deviates somewhat from that of an idealised octahedron. The ligand bite-angle is 74.6(3)°, which compares to 74.7, 74.3, and 72.3°, respectively, for the closely related complexes *fac*-[ReCl(CO)$_3$(L^2)],[2] *fac*-[ReBr(CO)$_3$(terpy)][20] and *cis*-[Mo(CO)$_4$(L^3)][3] {L^2 = 2,6-bis[(4*S*)-methyloxazolin-2-yl]pyridine, L^3 = 2,6-bis[(4*S*)-isopropyloxazolin-2-yl]pyridine, terpy = 2,2′ : 6′,2″-terpyridine}. There is a corresponding increase in the C(40)–Re–O(1) and C(20)–Re–N(1) angles to 97.3(8) and 104.3(5)°, respectively. There are no significant steric interactions between the metal moiety and the ligand; the shortest non-bonding distance is 3.03 Å [O(3) · · · C(20)].

The co-ordinated oxygen atom [O(1)] is close to planar (sum of angles 351.7°) indicating that it tends *towards* sp^2 hybridisation; the dihedral angle between the planes containing C(2)–O(1)–C(5) and Re–O(1)–C(5) is 29.3°. The co-ordinated and pendant acetal rings differ little and both are highly puckered; maximum deviations from the mean planes are 0.228 Å [O(2)] and 0.222 Å [O(3)] for the co-ordinated and pendant rings, respectively.

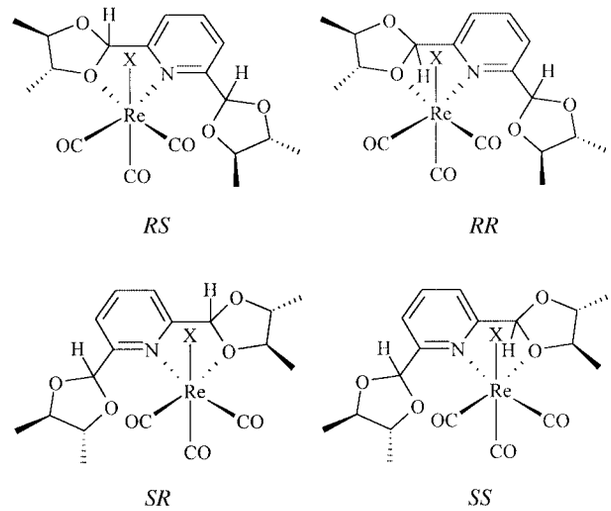

Fig. 2 The four possible diastereoisomers of the complexes [ReX(CO)$_3$(L^1)]. The letters refer to the configuration at the metal and at the acetal-carbon atom of the co-ordinated acetal ring, respectively.

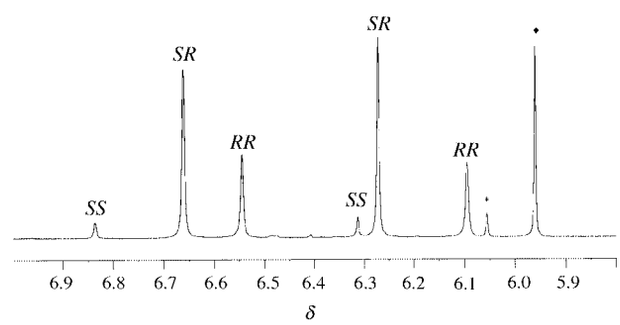

Fig. 3 Hydrogen-1 NMR spectrum of [ReBr(CO)$_3$(L^1)] at 298 K in $(CDCl_2)_2$, showing the acetal-CH region. See Fig. 2 for labelling of diasteroisomers. The signals denoted ◆ and * are due to the solvent and a minor impurity species, respectively; the impurity is not involved in any of the chemical exchange processes.

NMR studies

Ambient temperature (298 K) ^{1}H NMR spectra of the complexes, [ReX(CO)$_3$(L^1)] (X = Cl, Br or I), in $(CDCl_2)_2$ displayed well resolved signals due to the presence of three of the four possible diastereoisomers depicted in Fig. 2.[7] The spectra of all three complexes were similar and the results for [ReBr(CO)$_3$(L^1)] will serve to illustrate the analysis of the problem.

The ^{1}H NMR spectrum of [ReBr(CO)$_3$(L^1)] at 298 K comprised two regions of principal interest: (i) the acetal-CH region (*ca.* δ 6.0–6.9) and (ii) the methyl region (*ca.* δ 1.2–1.7). The acetal-CH region displayed three pairs of singlets of widely differing intensity, indicating the presence of three solution-state species (see below). The methyl region displayed twelve overlapping doublets ($^3J_{HH} \approx 6$ Hz); each of the three observed species gives rise to four doublets of equal intensity. The spectrum also displayed signals in the regions δ 3.5–4.6 and 7.4–8.4 due to the acetal ring and pyridine ring hydrogen nuclides, respectively. The signals in these regions overlapped extensively frustrating complete assignment and accurate measurement of the NMR parameters. Hydrogen-1 NMR data for the complexes [ReX(CO)$_3$(L^1)] (X = Cl, Br or I) are reported in Table 3 and the spectrum of [ReBr(CO)$_3$(L^1)] is shown in Fig. 3.

If inversion of configuration at the co-ordinated oxygen atom is assumed to be rapid on the NMR chemical shift timescale, the solution-state species can be assigned to three of the four possible diastereoisomers depicted in Fig. 2. The assump-

Table 3 Hydrogen-1 NMR data[a] for the complexes $[ReX(CO)_3(L^1)]$

Compound	Diastereoisomer[b]	$\delta(CH_3)$[c,d]	δ(acetal ring-H)[e]	δ(acetal-CH)	δ(pyridine-H)[e]
$[ReCl(CO)_3(L^1)]$	*SR* (65)	1.60(6.1), 1.36(6.0), 1.36(6.0), 1.32(6.1)	3.5–4.5	6.70, 6.34	7.5–8.2
	RR (29)	1.47(6.0), 1.43(5.9), 1.31(6.0), 1.29(6.3)		6.17, 6.55	
	SS (6)	1.51(6.2), 1.40(6.0), 1.39(6.4), 1.35(6.0)		6.37, 6.87	
$[ReBr(CO)_3(L^1)]$	*SR* (62)	1.59(6.1), 1.36(6.0), 1.35(5.9), 1.33(6.1)	3.6–4.6	6.66, 6.27	7.5–8.3
	RR (32)	1.46(6.0), 1.43(6.0), 1.32(6.0), 1.31(6.7)		6.10, 6.54	
	SS (6)	1.49(6.1), 1.40(6.0), 1.39(6.3)		6.31, 6.84	
$[ReI(CO)_3(L^1)]$	*SR* (67)	1.57(6.0), 1.36(6.0), 1.34(5.9), 1.34(≈7)	3.6–4.6	6.61, 6.22	7.5–8.1
	RR (29)	1.43(6.0), 1.43(6.1), 1.33(5.8), 1.30(6.0)		6.03, 6.56	
	SS (4)	1.47(6.2), 1.43(6.3), 1.38(5.9), 1.30(6.0)		6.27, 6.77	

[a] Recorded in $(CDCl_2)_2$ solution at 298 K; chemical shifts quoted relative to $SiMe_4$ as an internal standard. [b] Populations (%) given in parentheses. [c] $^3J_{HH}$/Hz given in parentheses. [d] Not all bands resolved. [e] Chemical shifts and scalar couplings for each diastereoisomer not measured due to extensive overlap of signals (see text).

tion of rapid O inversion is supported by theoretical calculations that predict very low barriers[21,22] and by the crystal structure of $[ReBr(CO)_3(L^1)]$ (see above). This shows that the co-ordinated oxygen atom is nearly planar, indicating clearly that the ground-state geometry at O is close to the transition-state for pyramidal inversion,[23] suggesting a low barrier to inversion.

The assignment of the major solution-state species was based on the crystal structure of $[ReBr(CO)_3(L^1)]$ (see above). In the solid-state, crystalline $[ReBr(CO)_3(L^1)]$ exists exclusively as the *SR* diastereoisomer (letters refer to the configuration at the metal and acetal-carbon atom of the co-ordinated acetal ring, respectively). Crystals of $[ReBr(CO)_3(L^1)]$ were dissolved in $CDCl_3$ at 213 K and the NMR spectrum acquired immediately (at 213 K). The spectrum shows the presence of a single diastereoisomer, presumably *SR*, which remains as the dominant species after equilibration. The *SR* diastereoisomer was thus assigned as the major solution-state species. Bands due to the two other diastereoisomers appear in the NMR spectrum after only a few minutes. The assignment of the other diastereoisomers was based on the results of the DNMR experiments (see below).

Three distinct dynamic processes are expected[2,3,7] [all of which are observed (see below)], namely (i) exchange of pendant and co-ordinated acetal rings *via* a *tick-tock* mechanism, (ii) *flip* of the co-ordinated acetal ring, and (iii) exchange of pendant and co-ordinated acetal rings *via* a *rotation* mechanism. The *tick-tock* process (Fig. 4a) leads to inversion of configuration at the metal and *may* also lead to inversion of configuration at the acetal-carbon atom of the co-ordinated ring. The acetal *ring flip* process (Fig. 4b) leads to formal inversion of configuration at the acetal-carbon atom, but not at the metal. Finally, although the rotation mechanism (Fig. 4c) could, in principle, lead to diastereoisomerisation (as a result of formal inversion of configuration at the acetal-carbon atom), this is not the case; exchange occurs between the pendant and co-ordinated acetal rings of each diastereoisomer (see below).

The *tick-tock* process is distinguished unambiguously from the *rotation* and *ring flip* fluxions because it leads to exchange of the 3- and 5-position hydrogen nuclides of the pyridine ring. Magnetisation transfer experiments (EXSY and selective inversion) at 298 K demonstrate clearly that exchange occurs initially between the acetal-CH nuclides of the *SR* diastereoisomer and the second most abundant species. The EXSY spectrum (Fig. 5) reveals that this process also leads to exchange of the 3- and 5-position pyridine-hydrogen nuclides of the two disateroisomers, at the same rate as the exchange of the acetal-CH nuclides. The rates of exchange measured using the EXSY technique are identical, within experimental error, to those measured using the selective inversion technique (see below). This shows clearly that the initial fluxional process is the *tick-tock* exchange of the pendant and co-ordinated acetal rings. Thus the configuration at the metal in the second diastereoisomer can be assigned as *R*. The configuration at the acetal-carbon of the co-ordinated acetal ring cannot be determined unambiguously. We tend to the view that it is likely to be *R*; geometric calculations indicate that the *RR* diastereoisomer is less sterically hindered than the *RS* diastereoisomer. The second species was thus assigned as the *RR* diastereoisomer.

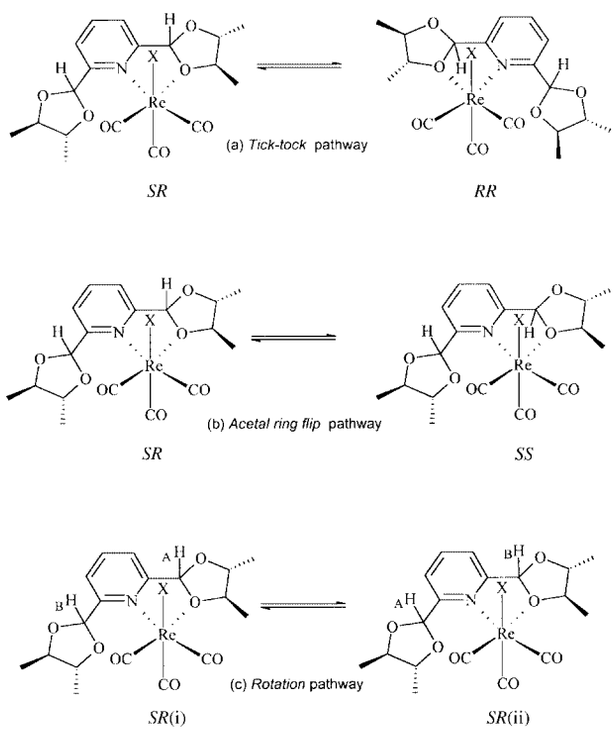

Fig. 4 The three different exchange processes in the complexes $[ReX(CO)_3(L^1)]$. Note that the rotation occurs in all three species and does not lead to any diasteroisomerisations; species (i) and (ii) are degenerate.

On warming further, EXSY experiments indicate the onset of a second fluxional process that leads to exchange between the *SR* diastereoisomer and the minor species. This is attributed to the acetal *ring flip*, since it does not lead to any additional magnetisation transfers between the 3- and 5-position pyridine-hydrogen nuclides. The minor species can thus be assigned as the *SS* diastereoisomer; *ring flip* leads to formal inversion of configuration at the acetal carbon, but not at the metal. The relative populations of the three species (Table 3), determined by integration of the acetal-CH signals, are in the order $SR > RR > SS$. This follows the trend expected from geometric calculations, which indicate that steric interactions between the co-ordinated acetal ligand and the metal moiety increase in the order $SR < RR < SS \approx RS$. In the case of the *RS* diastereoisomer, these steric interactions are sufficiently great to reduce

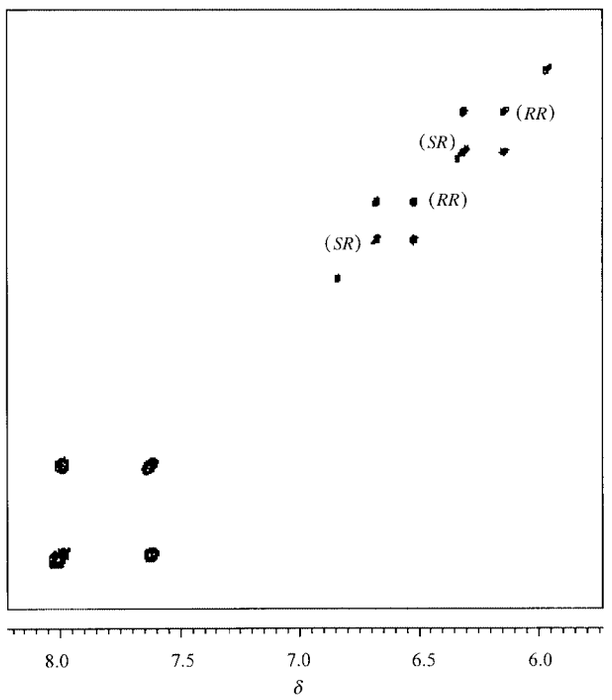

Fig. 5 Two-dimensional exchange spectrum of $[ReBr(CO)_3(L^1)]$ at 298 K (mixing time = 0.35 s) in $(CDCl_2)_2$. Exchange cross peaks are observed between the acetal-CH signals of the *SR* and *RR* diastereoisomers. Cross peaks are also observed between the 3- and 5-position pyridine-H signals (δ 7.5–8.3), showing clearly that exchanges are the result of the *tick-tock* fluxion.

its population below that which can be detected in the NMR experiment; hence the observation of only three of the four possible solution-state species.

Although it is only necessary to be able to assign one of the acetal-CH signals to a co-ordinated or pendant acetal ring, since all other assignments follow from the exchanges, this is problematic and no unambiguous assignment was possible. It is noteworthy that the co-ordination shifts of the *SR* diastereoisomer are the reverse of those of the *RR* and *SS* isomers; this is evident form the exchanges even though an unambiguous assignment of the acetal-CH signals to the pendant and co-ordinated rings is not possible. The different shifts are, presumably, due to the different shielding effects of the halogen and the carbonyl ligands. In the *SR* diastereoisomer the acetal-CH of the co-ordinated ring is oriented on the same side as the halogen, whereas in the *RR* and *SS* species the acetal-CH of the co-ordinated ring is oriented on the same side as the axial carbonyl ligand.

Dynamic NMR studies were performed on the three complexes, $[ReX(CO)_3(L^1)]$, in the temperature range 298–398 K. On warming, fully reversible band shape changes were observed in all regions of the spectra, but the acetal-CH signals are most amenable to analysis, so were used for the measurement of the exchange kinetics. A two-dimensional exchange (EXSY) spectrum at 298 K (Fig. 5) displayed cross peaks between the bands of the *SR* and *RR* diastereoisomers as a result of exchange between acetal rings *via* the *tick-tock* pathway (Fig. 4a).[2,3] The exchange kinetics were measured in the slow exchange regime using the selective inversion–recovery technique.[24–27] The signal due to one the acetal-CH signals of the *SR* diastereoisomer was selectively inverted at 298 and 303 K; magnetisation transfer to one of the acetal-CH signals of the *RR* diastereoisomer was clearly observed, enabling accurate rates to be measured. Experiments were repeated, inverting the other acetal-CH signal of the *SR* diastereoisomer; rates are identical within experimental error (±5–10%).

On warming further, the acetal-CH signals of the *SS* diastereoisomer also began to exhibit reversible broadening due to $SR \rightleftharpoons SS$ magnetisation transfers, resulting from the *flip* of the co-ordinated acetal ring[7] (Fig. 4b). Rates in the intermediate exchange regime were measured by total band shape analysis.[28] In solution, each diastereoisomer exists as a pair of degenerate species, depending on which of the two acetal rings is metal co-ordinated (see Fig. 4c), giving a total of twelve solution-state species, all of which must be considered. Since there are no scalar couplings between the pendant and co-ordinated acetal rings, this simplifies to the six-spin system problem shown below [letters in parentheses indicate the signals due to the pendant (p) and co-ordinated (c) acetal rings].

Spin system:	1	2	3	4	5	6
Assignments:	*SR*(c)	*SR*(p)	*RR*(c)	*RR*(p)	*SS*(c)	*SS*(p)
Rates:	k_{12}	k_{13}	k_{14}	k_{15}	k_{16}	
	k_{23}	k_{24}	k_{25}	k_{26}		
	k_{34}	k_{35}	k_{36}			
	k_{45}	k_{46}				
	k_{56}					

The variable temperature ^{1}H NMR spectra were simulated on this basis. At moderate temperatures (<363 K) spectra were simulated accurately using four non-zero rate constants (all other rates being negligible), namely k_{14} and k_{23} (*tick-tock*), and k_{15} and k_{26} (*acetal ring flip*). Above *ca.* 363 K it was also necessary to use non-zero rate constants for k_{12}, k_{34}, and k_{56} (*rotation*). Although the rates of *rotation* would be expected to be different for the three diastereoisomers, spectra were simulated using equal rates for the three processes, because of the problems of fitting the experimental spectra to a large number of independent variables. It seems unlikely that the energetics of the *rotation* differ greatly between diastereoisomers and the assumption is considered valid. Sixteen spectra were simulated, six of which are shown in Fig. 6.

The rate data measured by the band shape analyses and selective inversion experiments were used to determine the activation parameters from a least-squares fitting of the linearised Eyring equation. Activation parameters for the complexes, $[ReX(CO)_3(L^1)]$ (X = Cl, Br, I) are reported in Table 4.

Fluxional behaviour. Analysis of the variable temperature ^{1}H NMR spectra of the complexes $[ReX(CO)_3(L^1)]$ (see above) shows clearly that three independent fluxional processes (depicted in Fig. 4) are occurring; these are discussed below.

The *tick-tock* fluxion can be distinguished from the *ring flip* and *rotation* fluxions by virtue of the fact that the *tick-tock* process causes exchange of the 3- and 5-position pyridine-H nuclides. Thus the initial rate process can be attributed unambiguously to the *tick-tock* exchange of the pendant and co-ordinated acetal ring (see above). The free energies of activation for the *tick-tock* fluxion are in the narrow range 72–73 kJ mol^{-1} and show only minimal halide dependence. The magnitudes of $\Delta G^{\ddagger}$ (298 K) are similar to those measured for the tricarbonylrhenium(I) halide complexes of L^2,[2] but are lower than those of L^3.[3] The factors that affect fluxional energetics are complex and the origin of the barrier in the *tick-tock* fluxion is not entirely clear; electronic and geometric factors must both contribute. The *tick-tock* fluxion is presumably initiated by the interaction of one of the donor atoms on the pendant ring with the metal centre. The energetics will presumably reflect the ease of interaction of the pendant ring with the metal and the strength of the metal–donor atom bond of the co-ordinated ring. The molecular structures of $[ReX(CO)_3(L^1)]$ (see above) and $[ReX(CO)_3(L^2)]$[2] show that the ligands are geometrically similar (*e.g.* ligand bite angles are identical within experimental error) and there are no significant steric interactions between the ligands and the metal centre in either case. It therefore seems reasonable to conclude that the Re–O(acetal) and Re–N(oxazoline) bond strengths are approximately equal in these

Table 4 Eyring activation parameters[a] for the complexes $[ReX(CO)_3(L^1)]$

Complex	Process	$\Delta H^{\ddagger}$/kJ mol^{-1}	$\Delta S^{\ddagger}$/J mol^{-1} K^{-1}	$\Delta G^{\ddagger}$/kJ mol^{-1}
$[ReCl(CO)_3(L^1)]$	Tick-tock	76.95(0.85)	15.73(2.55)	72.27(0.09)
	Rotation	75.26(2.10)	[b]	83.33(0.37)
	Ring flip	70.71(0.77)	−21.87(2.31)	77.23(0.08)
$[ReBr(CO)_3(L^1)]$	Tick-tock	74.76(0.53)	7.60(1.56)	72.49(0.06)
	Rotation	81.82(6.29)	[b]	88.12(1.32)
	Ring flip	71.55(1.09)	−19.76(3.24)	77.44(0.12)
$[ReI(CO)_3(L^1)]$	Tick-tock	75.75(0.78)	9.47(2.29)	72.93(0.10)
	Rotation	104.14(12.63)	[b]	89.96(2.66)
	Ring flip	75.05(1.98)	−11.02(5.88)	78.33(0.23)

[a] Errors given in parentheses; $\Delta G^{\ddagger}$ reported at 298 K. [b] Data not reported (unreliable values due to narrow temperature range).

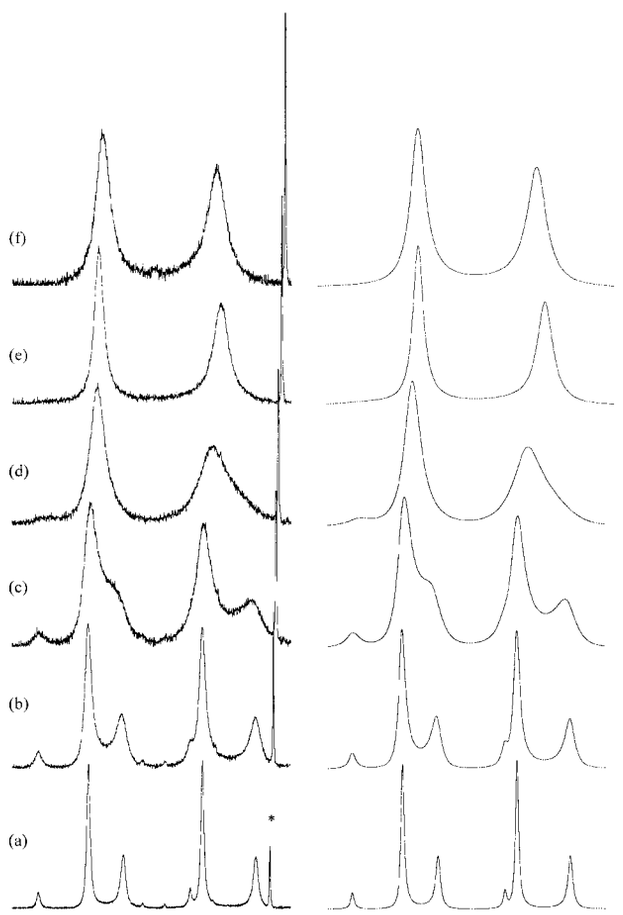

Fig. 6 Experimental and computer simulated variable temperature ^{1}H NMR spectra of $[ReBr(CO)_3(L^1)]$. (a) $T = 318$ K, $k_{tick\text{-}tock} = 9.0$, $k_{flip} = 1.2$, $k_{rotation} = 0.0$ s; (b) $T = 328$ K, $k_{tick\text{-}tock} = 20.0$, $k_{flip} = 3.0$, $k_{rotation} = 0.0$ s; (c) $T = 338$ K, $k_{tick\text{-}tock} = 45.0$, $k_{flip} = 6.5$, $k_{rotation} = 0.0$ s; (d) $T = 348$ K, $k_{tick\text{-}tock} = 110$, $k_{flip} = 13.0$, $k_{rotation} = 0.0$ s; (e) $T = 363$ K, $k_{tick\text{-}tock} = 330$, $k_{flip} = 33.0$, $k_{rotation} = 1.0$ s; (f) $T = 373$ K, $k_{tick\text{-}tock} = 650$, $k_{flip} = 65.0$, $k_{rotation} = 2.0$ s. See text for definition of rate constants. The signal labelled * is due to a minor impurity that is not involved in any of the exchange processes.

complexes. This is supported by the fact that the energetics of the *rotation* mechanism are also similar in these complexes (see below).

The *flip* of the acetal ring leads to inversion of configuration at the acetal-carbon atom of the co-ordinated acetal ring. The two possible mechanisms proposed previously for the acetal *ring flip*[7] are depicted in Fig. 7. Mechanism (i) involves cleavage of the Re–O bond, yielding a five co-ordinate transition state, followed by formation of a new Re–O bond. Mechanism (ii) involves loosening of the Re–O bond, concomitant with the formation of a pseudo seven-co-ordinate transition state. Previously it had been concluded (tentatively) that mechanism (i) was the most likely because of the relatively high barriers observed for the *ring flip* in the complexes $[ReX(CO)_3(L^4)]$ {X = Cl, Br or I; L^4 = 2-[(4*R*,5*R*)-dimethyl-1,3-dioxan-2-yl]-pyridine}.[7] If this were the mechanism, one might expect the acetal *ring flip* and *rotation* mechanisms to have similar barrier heights (since both would involve Re–O bond cleavage), which is clearly not the case; barrier heights for the *rotation* are *ca.* 6–11 kJ mol^{-1} greater than for the *ring flip* (Table 4). This suggests that mechanism (ii), which involves loosening, rather than cleavage, of the Re–O bond is operative. This is consistent with the low entropies of activation observed for both series of complexes (Table 4 and ref. 7). It is also noteworthy that the absolute magnitudes for the *ring flip* barrier in the complexes of L^1 are 8–11 kJ mol^{-1} less than in the complexes of L^4.[7] It may be that the presence of the pendant acetal ring modifies the mechanism of the *ring flip* (see above), but this is considered unlikely. The lowering of the free energy of activation for the acetal *ring flip* in the complexes of L^1 is presumably a direct consequence of the *tick-tock* fluxion loosening the Re–O interaction.

Like the *tick-tock* process, the *rotation* mechanism[2,3] (Fig. 4c) leads to exchange of the pendant and co-ordinated acetal rings. This could be accompanied by the formal inversion of configuration at the acetal-carbon of the co-ordinated acetal ring, but analysis of the DNMR line shapes indicates that this is not the case. Line shapes could only be simulated accurately assuming the exchange occurs without diastereoisomerisation. The free energies of activation (Table 4) are similar to those observed previously for analogous process in the tricarbonylrhenium(I) halide complexes of the bis(oxazoline) 2,6-bis[(4*S*)-methyloxazolin-2-yl]pyridine (L^2), namely $[ReX(CO)_3(L^2)]$ (X = Cl, Br or I).[2] The principal contribution to $\Delta G^{\ddagger}$ is presumably the energy required to break the Re–O(acetal) bond, which is necessarily cleaved. The similar magnitudes for the free energies of activation thus indicate that the Re–O(acetal) and Re–N(oxazoline) bond strengths are similar in these complexes. The halide dependence on the energetics of the *rotation* appears significant and may be due in part to the increasing size of the halide, but is more likely a consequence of the narrow temperature range over which the kinetics were measured. The moderately large errors associated with the activation parameters are also due to the narrow temperature range.

Conclusion

The ligand, 2,6-bis[(4*R*,5*R*)-dimethyl-1,3-dioxan-2-yl]pyridine (L^1) complexes to the halogenotricarbonylrhenium(I) metal moieties in a bidentate fashion *via* the pyridine N atom and an O atom of one of the acetal rings. The resultant compounds, $[ReX(CO)_3(L^1)]$ (X = Cl, Br or I), undergo three independent fluxional processes, namely exchange of the pendant and co-ordinated acetal rings by *tick-tock* and *rotation* mechanisms, and a *flip* of the co-ordinated acetal ring. Rates of the stereodynamics were measured in the slow and intermediate exchange regimes by selective inversion experiments and standard band shape analysis, respectively. The free energies of activation for

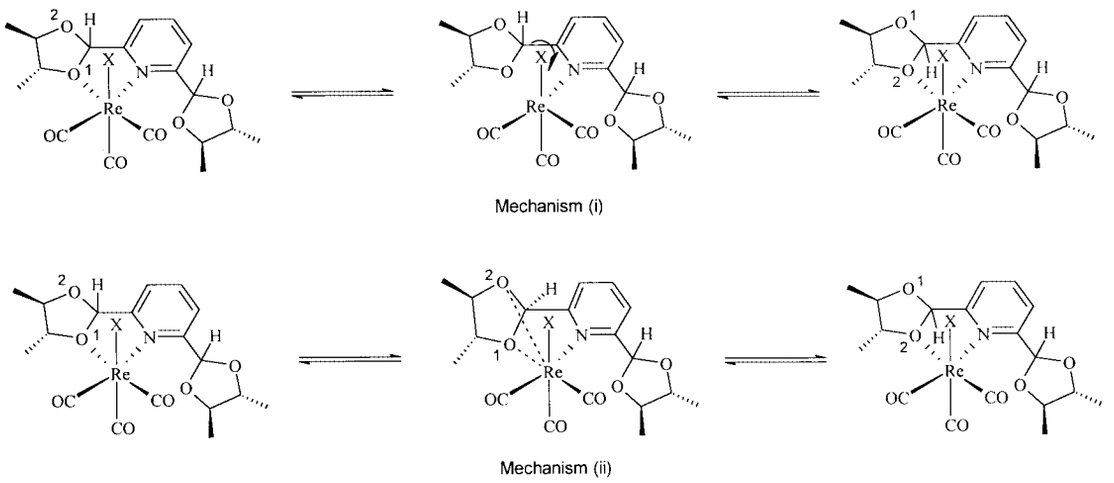

Fig. 7 The two possible mechanisms proposed for the acetal ring flip fluxional process.

the *tick-tock* and *rotation* fluxions are close to those measured previously for the related bis(oxazoline) complexes, [ReX(CO)$_3$(L^2)] {X = Cl, Br or I; L^2 = 2,6-bis[(4*S*)-methyloxazolin-2-yl]pyridine}. The mechanism of the acetal *ring flip* remains a matter of conjecture, but results reported here point towards a mechanism that involves both oxygen atoms of the acetal ring being loosely bound to the metal in the transition state, contrary to our previous results.[7]

Acknowledgements

Birkbeck College, McMaster University, University College London and the Natural Science and Engineering Research Council of Canada (NSERC) are acknowledged for financial assistance.

References

1 E. W. Abel and K. G. Orrell, in *Encyclopaedia of Inorganic Chemistry*, ed. R. B. King, Wiley, New York, 1994, vol. 5, pp. 2581–2615.
2 P. J. Heard and C. Jones, *J. Chem. Soc.*, *Dalton Trans.*, 1997, 1083.
3 P. J. Heard and D. A. Tocher, *J. Chem. Soc.*, *Dalton Trans.*, 1998, 2169.
4 E. W. Abel, N. J. Long, K. G. Orrell, A. G. Osborne, H. M. Pain and V. Šik, *J. Chem. Soc.*, *Chem. Commun.*, 1992, 303.
5 E. R. Civitello, P. S. Dragovich, T. B. Karpishin, S. G. Novick, G. Bierach, J. F. O'Connell and T. D. Westmoreland, *Inorg. Chem.*, 1993, **32**, 237.
6 A. Gelling, M. D. Olsen, K. G. Orrell, A. G. Osborne and V. Šik, *J. Chem. Soc.*, *Dalton Trans.*, 1998, 3479 and refs. therein.
7 P. J. Heard, A. D. Bain and P. Hazendonk, *Can. J. Chem.*, in the press.
8 D. D. Perrin and W. L. F. Armarego, *Purification of Laboratory Chemicals*, Pergamon, Oxford, 1998.
9 S. P. Schmidt, W. C. Trogler and F. Basolo, *Inorg. Synth.*, 1979, **28**, 160.
10 F. A. J. Meskens, *Syntheses*, 1981, 501.
11 A. D. Bain and G. J. Duns, *Can. J. Chem.*, 1996, **74**, 819.
12 A. D. Bain and J. A. Cramer, *J. Magn. Reson.*, 1996, **118**, 21.
13 G. Binsch and H. Kessler, *Angew. Chem.*, *Int. Ed. Engl.*, 1980, **19**, 411.
14 E. W. Abel, T. P. J. Coston, K. G. Orrell, V. Šik and D. Stephenson, *J. Magn. Reson.*, 1986, **70**, 34.
15 G. Schaftenaar, Molden v3.6, CAOS/CAMM Centre, University of Nijmegen, 1999.
16 G. M. Sheldrick, SHELXL 93, University of Göttingen, 1993.
17 D. A. Edwards and J. Marshalsea, *J. Organomet. Chem.*, 1977, **131**, 73.
18 E. W. Abel, K. Kite and P. S. Perkins, *Polyhedron*, 1987, **6**, 319 and refs. therein.
19 E. L. Eliel and S. H. Wilen, *Stereochemistry of Organic Compounds*, Wiley, New York, 1994.
20 E. W. Abel, V. S. Dimitrov, N. J. Long, K. G. Orrell, A. G. Osborne, H. M. Pain, V. Šik, M. B. Hursthouse and M. A. Mazid, *J. Chem. Soc.*, *Dalton Trans.*, 1993, 597.
21 W. Cherry and N. Epiotis, *J. Am. Chem. Soc.*, 1976, **98**, 1135.
22 R. F. W. Bader, J. R. Cheeseman, K. E. Laidig, K. B. Wiberg and C. Breneman, *J. Am. Chem. Soc.*, 1990, **112**, 6530.
23 E. W. Abel, S. K. Bhargava and K. G. Orrell, *Prog. Inorg. Chem.*, 1984, **32**, 1.
24 A. D. Bain and J. A. Cramer, *J. Phys. Chem.*, 1993, **97**, 2884.
25 A. D. Bain and J. A. Cramer, *J. Magn. Reson.*, *Ser. A*, 1993, **103**, 217.
26 S. Forsen and R. A. Hoffman, *J. Chem. Phys.*, 1963, **39**, 2892.
27 R. E. Hoffman and S. Forsen, *Prog. Nucl. Magn. Reson. Spectrosc.*, 1966, **1**, 15.
28 J. Sandström, *Dynamic NMR Spectroscopy*, Academic Press, New York, 1982.

Paper 9/04026I